Dynamic behaviors for a hybrid leg-wheel mobile platform

C. Steeves[1], M. Buehler[1], S.G. Penzes[2]

[1]McGill University, Center for Intelligent Machines, Ambulatory Robotics Lab, 3480 University Street, Montreal, QC, Canada, H3A 2A7
[2]Defence R&D Canada, Defence Research Establishment Suffield (DRES), Box 4000 Medicine Hat, AB, Canada T1A 8K6

ABSTRACT

A hybrid platform for an Unmanned Ground Vehicle (UGV), one with legs and wheels, was initially considered to yield a design that possessed a high degree of intrinsic mobility. Integrating a high level of mobility reduces the UGV's perception and computational requirements for successful semi-autonomous or autonomous terrain negotiation. An investigation into the dynamic capabilities of the hybrid design revealed a large amount of otherwise impossible behaviors. The widened scope of maneuvers enabled the simulated robot to negotiate higher obstacles, clear larger ditches and generally improved its rough terrain mobility. A scalability study was also undertaken to predict dynamic potential of various platform sizes and to aid in the selection of design specifications such as motor torque-speed curves. The hybrid design of the platform (legs with active wheels) proved invaluable in achieving these dynamic behaviors and revealed that the leg-wheel design was as fundamental to dynamic capabilities, as it was to intrinsic mobility.

Keywords: Dynamic, hybrid, legged, wheeled, leg-wheel, unmanned, robotic, intrinsic, mobility, compliance

1. INTRODUCTION

A hybrid design for ANT, one with wheels at the end of 1 DOF legs, was initially considered for development due to its intrinsic mobility [1]. Prior to the dynamic study presented in this paper, this mainly involved investigating the benefits associated with the addition of legs to a wheeled platform. Improvements in obstacle negotiation and increased slope or traction control are examples of this type of mobility benefit. The addition of legs also enabled walking gaits and with the addition of compliance to the legs (sprung prismatic legs), such gaits as bounding were also possible (see Figure 1).
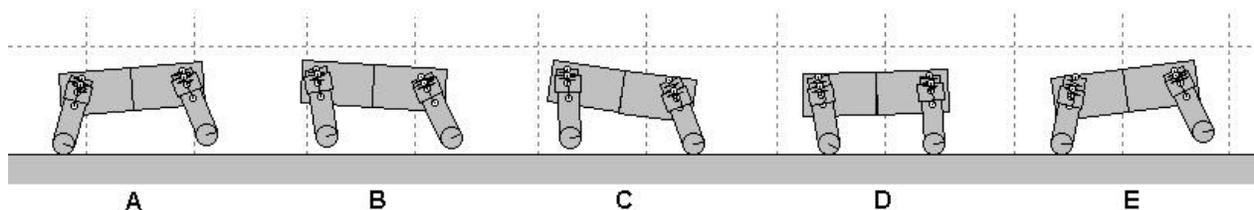

Figure 1. Bounding gait with locked wheels

However, when further investigation into feasible dynamic behaviors was undertaken, the evaluation of this hybrid platform was redirected. It became a study that accentuated the benefits associated with the addition of wheels to a legged platform. This paper presents some of the dynamic possibilities made apparent by this study, none of which would be possible without the addition of the wheels.

2. MODEL DEVELOPMENT

Prior to the dynamic study, a scalability study was done to assess the performance of various *scaled* sizes of the platform. The techniques developed to parameterize realistic models for this scalability study were implemented in the dynamic investigation. The scalability study involved six-legged platforms, but the parameters were adjusted to yield four-legged platforms as used in the dynamic study.

The reasoning behind the different number of legs used by the two studies lies in the modularity of the platform [1, 2]. It was designed to operate with a minimum of two segments (4 legs) with the ability to add extra segments, each containing two legs. For more static behaviors, a six-legged platform was used quite frequently owing to the inherent stability created by the extra pair of legs [4,5,6]. However, for the dynamic maneuvers, it was found advantageous to use only the first two segments. Only using two segments was beneficial because it enables the robot to pitch its body when supported by only one set of legs. This is owing to the shorter body length of the two-segment module, which with the same length legs can enables the robot to reach past its body's center of mass. Simply removing the middle pair of legs from the 6-legged platform would not have enabled this type of behaviour, thus reemphasizing the benefits of modularity.

Two existing six-legged platforms were used as baselines (or *control* models) for scaling to other sizes. The first was DRES's original ANT (see Figure 2) [1], which was modified in simulation to have longer legs, smaller wheels and compliant legs. The second was the robotic hexapod, RHex (see Figure 3) [4,5], enhanced with active wheels. These two platform's parameters can be compared below in Table 1.
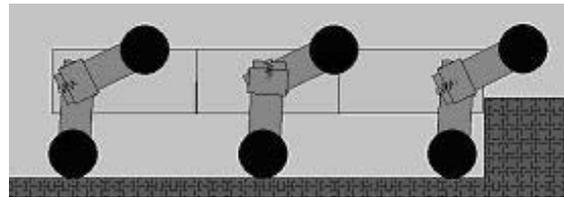

Figure 2. The DRES Articulated Navigation Testbed (ANT) with 4 legs (left) and the modified 6-legged version used in simulation (right)

Figure 3 RHex, a six-legged walking (left) and running (right) robot with compliant legs

Table 1. Parameters for each control model

Parameter Description	ANT	RHex
Body Length (m)	**3.380**	**0.400**
Body thickness (m)	0.500	0.120
Body width (m)	1.250	0.090
Body Volume (m^3)	2.113	0.004
Leg length (m)	0.800	0.160
Ground Clearance	0.500	0.100
Body Density (kg/m^3)	645.2	1736.0
Mass (Kg)	1362.99	7.50
Power Density (Nm/Kg)	1.368	0.730
Hip Torque	1864.6	5.5
Hip No Load Speed (rpm)	58.2	303.0
Wheel Torque (Nm)	279.9	5.5
Wheel No Load Speed (rpm)	260.1	303.0

Table 2 outlines the methods chosen to scale each parameter. The order in the table reflects the computational order of the parameters (i.e. volume appears before mass because the calculation of mass requires the body volume). The remaining dimensions were simply geometrically scaled using the ratios and relationships given in Table 3.

Table 2. Parameter computation

Parameter Description	Method of Computation
Body Length (INPUT)	0.4m to 3.38 m (RHex to ANT)
Body Thickness	Linearly Interpolated (RHex to ANT) as a percentage of Body Length
Body Width	Linearly Interpolated (RHex to ANT) as a percentage of Body Length
Body Volume	Body Length × Body Thickness × Body Width
Leg Length	Linearly Interpolated (RHex to ANT) as a percentage of Body Length
Ground Clearance	Leg Length – (Body Thickness)/2
Body Mass Density	Linearly Interpolated (RHex to ANT) as a percentage of Body Length
Body Mass	Body Volume × Body Mass Density
Power Density (Hip Torque/Body Mass)	Linearly Interpolated (RHex to ANT) as a percentage of Body Length
Hip Torque	Body Mass × Power Density
Hip No Load Speed	Linearly Interpolated (RHex to ANT) as a percentage of Hip Torque
Wheel Torque	Linearly Interpolated (RHex to ANT) as a percentage of Hip Torque
Wheel No Load Speed	Linearly Interpolated (RHex to ANT) as a percentage of Hip Torque

Table 3. Geometrically scaled parameters

Parameter Description	Method of Computation
Leg Slider Length	(Torso Thickness) × 2/5
Leg Width	(Torso Thickness) × 1/2
Leg Slider Width	Leg Width × 6/5
Hip Displacement on body	Leg Slider Length
Wheel Diameter	Leg Width

Since the existing RHex platform had no wheels, RHex's hip motor specs were used as stand-ins for RHex's wheel motors. The hip actuation was sufficient to accomplish the wheel actuation's tasks and was chosen as a preliminary estimate in order to start the study. Following this dynamic study, investigation into the required performance of wheel actuation was undertaken. The no load speed was taken as the minimum speed required so as not to inhibit the dynamic maneuvers performed with a passive wheel. The stall torque was chosen based upon the necessity that the platform be able to use its wheels to drive up an incline of at least 45 degrees. The minimum requirements found with this more precise manner were found to be very close to the preliminary estimate of using the hip motors. Thus, the original estimate was more than an adequate estimate to begin simulating behaviors.

The dynamic capability of the ANT platform was investigated using a model with body length of 1 meter from the scalability study. The parameters used to model the 4-legged version of the 1-meter model are tabulated in Table 4, adjacent to the 6-legged scaling results. A 1-meter model was both small enough to exhibit inherent dynamic capability and large enough to traverse practical sized obstacles. A smaller model would have demonstrated larger dynamic performance, but would have been less practical in terms of obstacle negotiation and payload capacity.

Table 4. Scaled model parameters

Parameter Description	6 - legged	4 - legged
Body Length (m)	**1.000**	**0.667**
Body thickness (m)	0.197	0.197
Body width (m)	0.324	0.324
Body Volume (m^3)	0.064	0.0424
Leg length (m)	0.289	0.289
Ground Clearance	0.181	0.181
Body Density (kg/m^3)	1516.4	1516.4
Mass (kg)	96.41	64.28
Hip Power Density (Nm/Kg)	0.858	0.858
Hip Torque	82.8	82.8
Hip No Load Speed (rpm)	292.8	292.8
Wheel Torque (Nm)	16.9	16.9
Wheel No Load Speed (rpm)	301.2	301.2

The wheel diameter was made equal to the leg width in this investigation to ensure the wheel would not inhibit any dynamic movements geometrically. The simulation model was adjusted accordingly to maintain the same ratio of leg length to ground clearance with this wheel diameter. Friction coefficients between the wheels and the ground were set to 0.9 and 0.8 (μ_s and μ_k) to approximate a rubber on clay interaction. As well, the coefficient of restitution was set to a value of 0.1 to approximate this same material interaction.

The dynamic behaviors highlighted in this report were simulated with a spring constant for each compliant leg of 10,000 Nm (with no damping). This value was chosen so that the robot would have a natural frequency of approximately 2 Hz. when bouncing freely. This standard frequency of 2 Hz. is a general rule of thumb used in dynamic robots of this size range and stems from the experience of the ARL [3]. It should be mentioned that there was a small amount of frictional dampening originating from the inelasticity of the tires and the compliance's slider-stops (rope). Any tire compliance was ignored largely owing to the assumption that the softer spring of the leg would be severely dominant in the dynamics.

The motors were assumed to have typical DC motor operating characteristics and thus a standard torque-speed curve was used. This generalized torque-speed curve, illustrated in Figure 4, only permits torques within the operating region (shaded area). No battery model was implemented, meaning the battery voltage was assumed to be unaffected by the motor currents (no battery internal resistance) and always able to deliver the nominal voltage to the motor. The motor driver's amplifiers were also considered ideal, that is, able to deliver the starting current or any other current sunk by the motor.
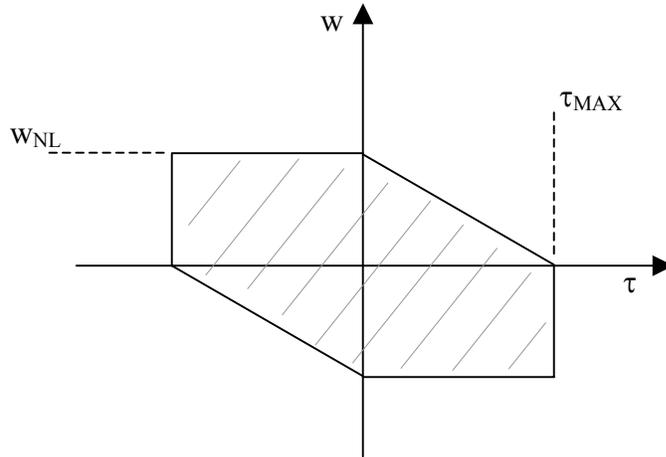
Figure 4. Generalized Torque-Speed Curve

To ensure that the behaviors in this study were realistic, the motors' parameters obtained using the scalability study were verified with manufacture's catalogues. Feasible motor and gearhead combinations are listed below for the hips and wheels.

Table 5. Motor Specifications

Hip Motors	
Motor	Gearhead
Maxon EC 60 (DC Brushless "Δ-circuit") Mech. Cont. Power: 400 W Stall Torque: 11.8 Nm No load Speed: 5000 rpm Weight: 2.45 Kg	*Maxon GP81* (Planetary Gearhead) Reduction: 14:1 Permissible Torque: 90 Nm Max. Efficiency: 75% Weight: 3 Kg
Wheel Motors	
Motor	Planetary Gear
Maxon RE 35 (DC Brushes)	*Maxon GP 42C*
Weight: 0.34 Kg	Weight: 0.36 Kg

The total weight of all eight motors and gearheads (4 hip, 4 wheel) is 24.6 Kg. This would make up 38% of the total weight of the robot. The remaining 40 Kg would be made up of batteries, structural components and electronic hardware. This mass ratio is typical for autonomous mobile robots. It should be mentioned that a smaller scale size was also developed in the same manner and is currently being constructed. All of the components for this smaller size have been selected, further supporting the validity of these scaled models and the methods used. Even batteries and motor drivers, selected as not to limit the motor's performance with saturation, are within desired weight and volume envelopes.

3. DYNAMIC BEHAVIORS

3.1 One leg bounce

This behaviour is a basic dynamic movement that utilizes the hybrid wheel-leg design and a first step to many other behaviors. The basic sequence of maneuvers is depicted in Figure 5. It repeatedly performs this sequence, each time gaining height, in roughly the same spot. However, actuation limitations restrict the maximum obtainable height as illustrated in the figure.
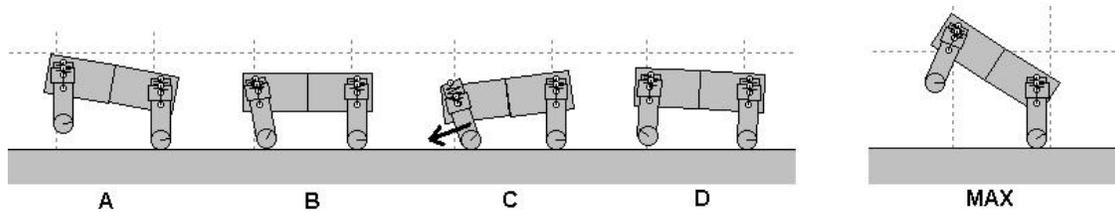
Figure 5. One leg bounce sequence

The leg that stays in contact with the ground has its wheel locked and always stays perpendicular to the ground. The other leg gives the energy required to increase the height through a couple of set point motions, while its wheel is allowed to roll freely. While falling downward this leg is set to an angle slightly towards the torso (see movement A and B). The moment the compliance begins to propel the robot back in the air, the leg is commanded to be perpendicular with the torso, as in movement C. This maneuver adds more energy to the robot than was stored in the compliance, hence the increase in height. If this is repeated, even with the same leg angle set point, each time the robot gains a small amount of height.

The free rolling wheel on the energetic leg allows the leg to add energy to the vertical motion of the robot, while roughly maintaining the same horizontal position (horizontal forces dissipated through the wheel). Without the free rolling wheel, the friction would slow the leg down and severely inhibit the dynamic capabilities of the robot. That is, if the leg cannot swing fast enough to cause a vertical displacement greater than that delivered by the compliance, then the leg will not add energy to the robot. This is the exact effect responsible for the maximum obtainable height. The higher the robot bounces, the more the compliance compresses and therefore the more acceleration the robot experiences. After a critical point, the motor's no-load speed restricts the robot from adding any more energy into the bounce.
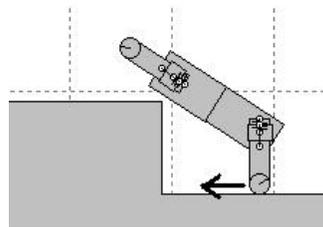

Figure 6. Obstacle clearance performed following one leg bounce

One of the maneuvers the robot can do, once it has reached the maximum height, is employing the wheel on the ground to drive the robot's body over an obstacle. This maneuver is illustrated in Figure 6.

3.2 Two leg bounce

This behavior is identical to the one leg bounce except that both legs are used for to supply the robot with vertical energy. The basic sequence of maneuvers, depicted in Figure 7, is repeatedly performed, each time gaining height in roughly the same spot. Just as in the one leg bounce, actuation limitations restrict the maximum obtainable height illustrated in Figure 8. Utilizing the wheels to actively aid the leg swing (Figure 7.C.) increased the maximum obtainable height or ground clearance, as well as enabled the wheel-assisted robot to reach an equivalent height quicker.

The two leg bounce is a good first step for any maneuver that would require a large initial ground clearance or a large amount of energy stored in the compliance (i.e. pronking). It is also a simple indicator of how the addition of active wheels increases the platform's performance.
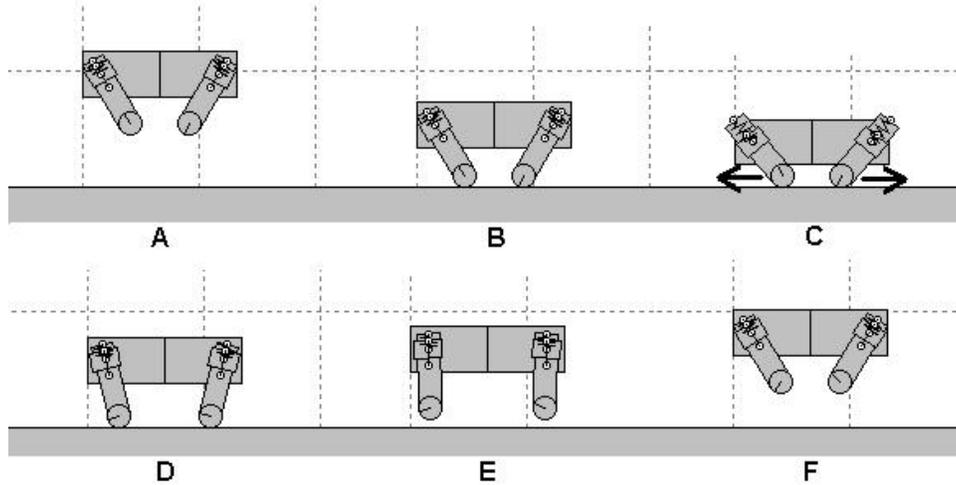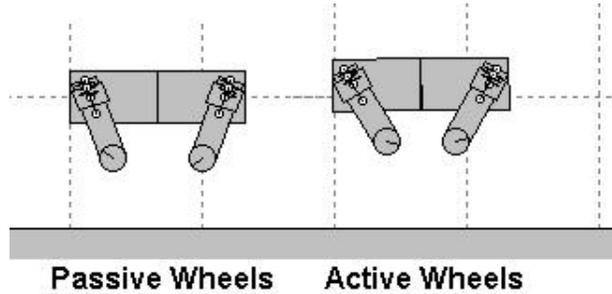
Figure 7. Two leg bounce sequence

Figure 8. Maximum height obtained for two leg bounce

3.3 Inverted pendulum control

This behaviour allows the robot to suspend its body in the air in a controlled manner. It begins with the one leg bounce and as soon as it's reached the maximum obtainable height, it performs the sequence of maneuvers depicted in Figure 9. The figure illustrates that as soon as the leg is in the air, the opposite wheel drives toward it, continuing to do so until the robot is vertical. This motion gives the robot the energy required to raise the torso in the air further than the one leg bounce controller.
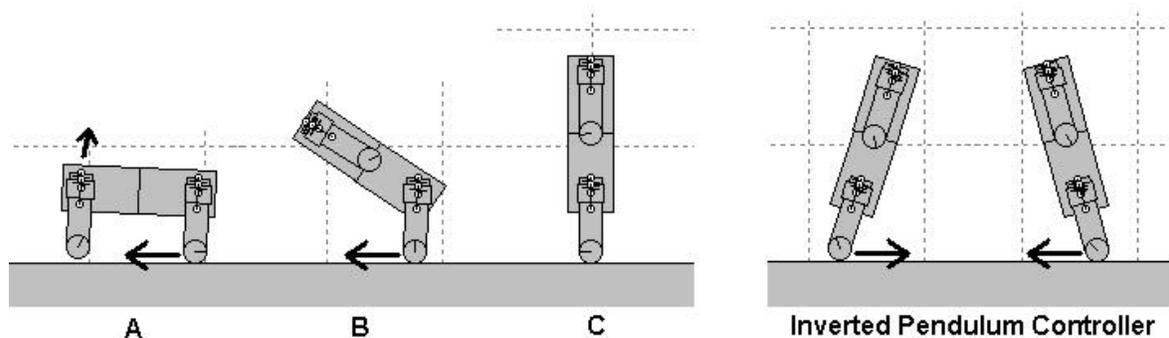
Figure 9. Inverted pendulum control

As soon as the torso is perpendicular to the ground, the bottom hip is locked and the inverted pendulum controller ensures that the torso remains suspended. Its set point, or desired position, is that illustrated in Figure 9.c. The corrective maneuvers are also illustrated in Figure 9. The controller basically obtains the desired wheel angle ($\theta_{DESIRED}$), and therefore the wheel torque, by adding/subtracting a *proportioned* angle to it's current one. This *proportioned* angle is related to the torso angle and is the basis of the PD controller used:

$$\theta_{DESIRED} = \theta_{CURRENT} + K_D(90 + \theta_{TORSO}) + K_V \dot{\theta}_{TORSO}$$

By setting the desired torso angle to one slightly offset from the 90 degrees depicted in Figure 9.C., the controller will drive the platform at a constant speed in the direction it is *leaning* towards. This will enable the robot to overcome obstacles in the manner previously illustrated in Figure 6, but in a much more controlled fashion.

3.4 One leg flip

This maneuver is depicted sequentially Figure 10. Initially, it follows the same sort of behaviour as the inverted pendulum controller. After the one leg bounce reaches its peak height, the wheel on the ground drives towards the body (movement A and B). Except, the wheel continues driving past the torso's vertical position and the top leg swings around 180 degrees (movement D to E). Around the position of D, the wheel breaks and allows the torso to fall back down. This stores energy in the leg (movement F), only to return it to the body, and then the other wheel drives towards the torso to start the flip in the other direction. Thus, positions A and K are roughly the same position.
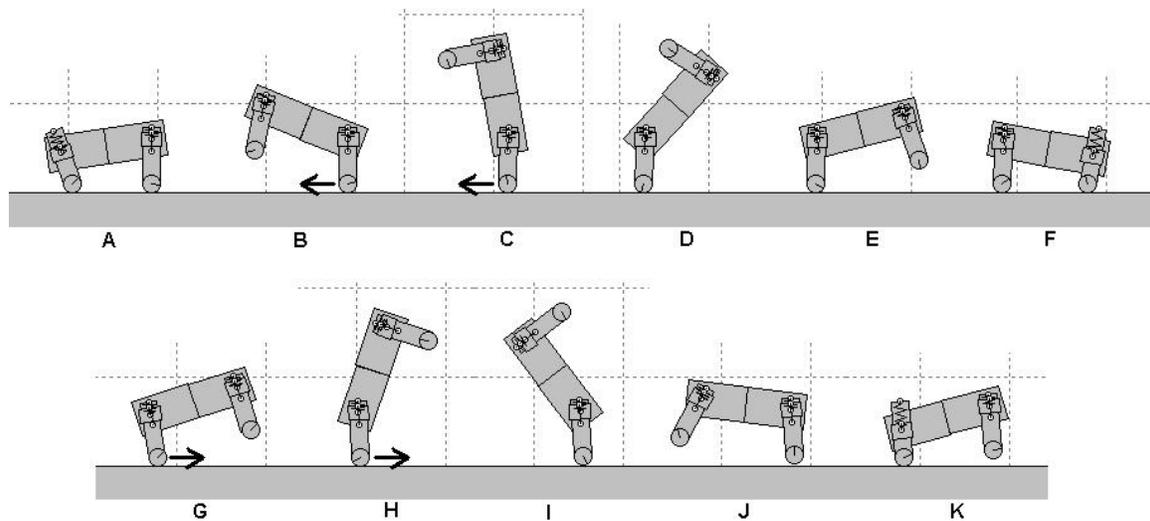

Figure 10. One leg flip sequence

Some interesting behaviors can be performed immediately following the sequence of movements illustrated in Figure 10. Such is the case for the maneuvers depicted in Figure 11. Notice that Figure 10.K. and Figure 11.A. are captured at the same moment in time, meaning Figure 11 is just a possible continuation of events from Figure 10. This type of continuation utilizes the energy stored in the compliance from the previous dynamic maneuver. Observe the very large amount of ground clearance that this maneuver yields in Figure 11.J.
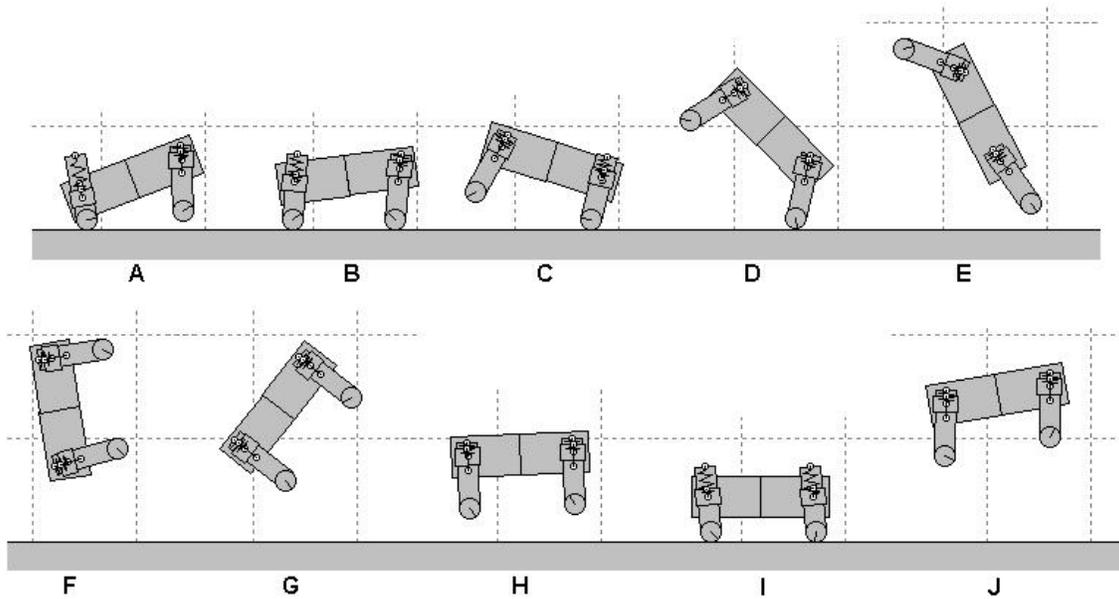
Figure 11. Forward flip after one leg bounce

3.5 Back flip

This maneuver is depicted sequentially Figure 12. The wheel at the end of the front/right leg (see Figure 12.A.) is left free to roll, while the wheel at the end of the rear/left leg is controlled. This allows the front leg to lift the front of the robot up in the air and the rear leg to control the amount of rotation the robot undergoes in the air. The rear wheel is passive normally and is active around maneuvers C and D. In Figure 12.D., the rotational effect on the direction of wheel activation is illustrated. Obviously, the amount of torque and duration of activation also play an important role in this situation.
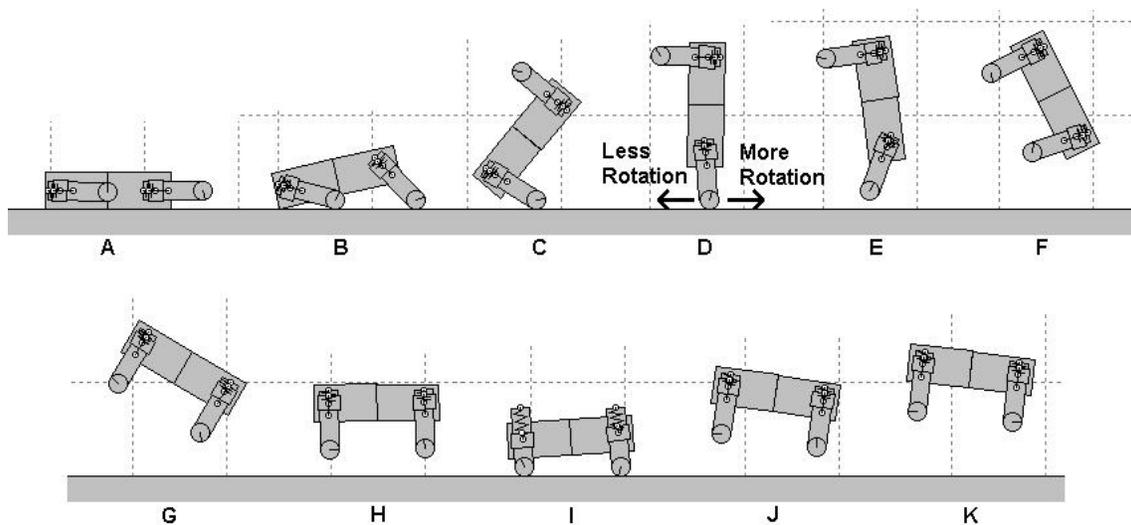

Figure 12. Back flip sequence

It should be mentioned that the back flip only causes a small horizontal displacement (rearward). The motion is a vertical displacement with a rotation, not one that pushes backward. In other words, it is a back flip and not a handspring.

As can be seen in Figure 12.K., the robot obtains a large amount of ground clearance after performing this maneuver. This height may also be used to perform various other dynamic behaviors, as it obtains this large amount of ground clearance much faster than with other maneuvers. In the sequence portrayed in Figure 12, both legs land roughly on the ground at the same time. However, if more or less rear wheel activation occurs, the front or rear leg land at different moments in time - creating even more dynamic opportunities.

Figure 13 illustrates using the back flip to get over a high step. It performs the same maneuvers as the regular back flip except that the robot initially drives towards the obstacle. The step simulated in Figure 13 is 0.45 m high, which is significantly taller than its ground clearance or the 0.25 m step that the 6-legged, 1 m ANT could negotiate in the scalability study. This highlights the clear advantage of exploiting the dynamic capabilities of the robot.
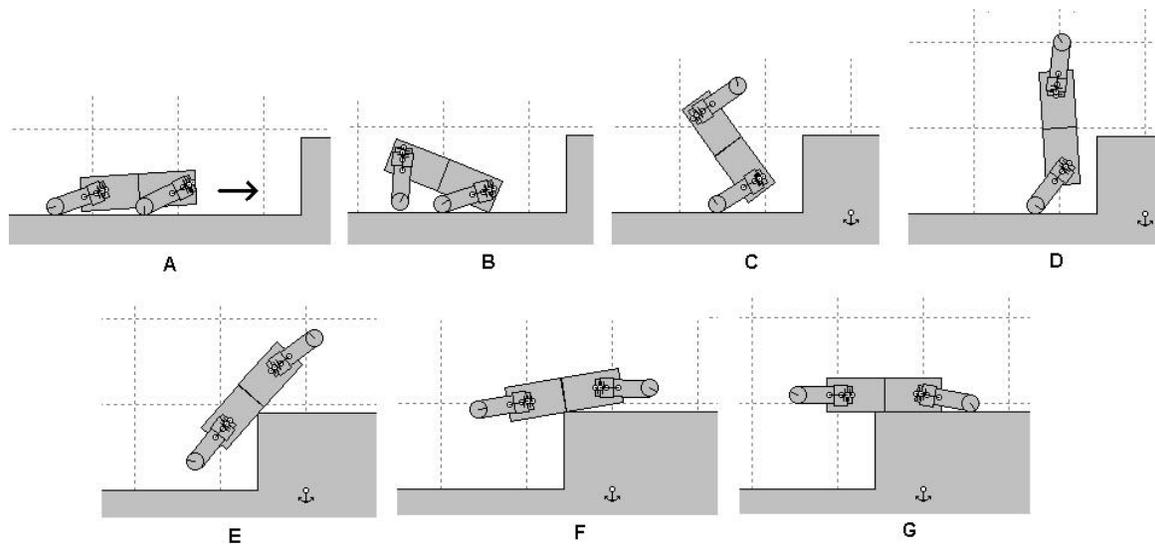

Figure 13. Driving towards a large step (0.45 m) and flipping onto the ledge

3.6 Pronk

This gait starts with the two leg bounce to obtain a large initial ground clearance. After it has obtained the maximum possible height, the sequence of maneuvers depicted in Figure 14 enables the robot to pronk. Upon touch down, the rear leg hits first because the rear legs are set at a smaller angle than the front. Immediately upon touchdown, the rear wheel drives the robot in the direction shown by the arrow in Figure 14.B. and the front wheel is set to passive. This not only gives the robot a forward velocity, but also aids to pitch the front end upwards. When the front leg's compliance reaches the bottom of its stroke (Figure 14.C.), the front legs swing towards the body with the assistance of the active front wheels (Figure 14.D.). This adds vertical energy to the robot and also aids to pitch the front end of the robot up. This front swing is the major motion that yields body pitch control for this pronking mode. Note that the rear leg does not swing during stance, a feat that is made possible only through the use of the wheels.
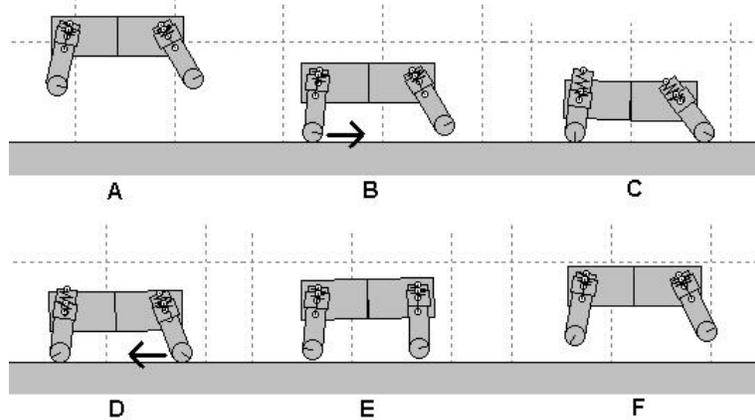
Figure 14. Pronking sequence reaching speeds over 1 m/s

As soon as lift-off is sensed, the wheels are locked and the legs are set to angles used for the next touchdown. As the robot's forward velocity increases, these set point angles of the legs are adjusted slightly to maintain the gait. After only rough tuning, speeds of over 1 m/s have been reached using this pronking mode, but with fine-tuning this speed is expected to increase.

The ground clearance is maintained even at the higher speeds owing to a couple of factors. Firstly, the wheels input most of the energy used to increase or maintain a forward velocity. Thus, the legs can solely be used to maintain the ground clearance and don't need to be used to input forward acceleration. Secondly, in a pronk the rear compliance always receives more than its share (half) of the energy needed to return the robot to the same height. This is a byproduct produced when the forward momentum added to the platform is displaced partially to the rear of the robot. Therefore any vertical energy lost during touchdown is more than adequately compensated for in the rear legs. With no need to use the rear leg to gain any height in the rear end of the robot, it can be set to a constant angle. The front leg can then be used solely to add the lost energy in the front to pitch the robot upwards, leveling the robot both in flight and at touchdown.

4. CONCLUSIONS

Dynamic behaviors have the potential to greatly enhance the mobility of ANT. This study focused on exploring some basic dynamic behaviors that can then be applied or modified to negotiate real-world obstacles. Maneuvers immediately following the aforementioned behaviors can be performed to utilize the dynamic energy that they yield. For example, the large ground clearance obtained from the forward flip (Figure 8.J.) could be harnessed to negotiate a high obstacle or to propel itself over a deep ditch. Maneuvers such as the back flip and the inverted pendulum were modified in this study to perform examples of such accomplishable tasks.

The existing ANT platform already has good mobility utilizing the hybrid concept of legs and wheels. With all the capable dynamic modes demonstrated in this report, the hybrid design continues to yield behaviors that would not otherwise be possible. These dynamic behaviors widen the scope of negotiable obstacles and generally increase the realm of mobility. As such, a smaller robot with intrinsic dynamic capabilities will outperform a larger robot without these arsenals. Given the benefits of this novel hybrid design, especially its strong dynamic capabilities, McGill's ARL is developing and testing this platform further. Currently, a smaller sized ANT (40 cm body length) is being constructed to test and validate the hybrid design.

ACKNOWLEDGMENTS

REFERENCES

1. C.A. Brosinsky, D.M. Hanna, and S.G. Penzes, "Articulated Navigation Testbed (ANT): an example of Adaptable Intrinsic Mobility", Proceedings of SPIE conference Unmanned Ground Vehicle Technology II, April 2000, Orlando, FL.
2. C.A. Brosinsky, S.G. Penzes, M. Buehler, C. Steeves., "Integrating Intrinsic Mobility into Unmanned Ground Vehicle Systems", Proceedings of SPIE conference Unmanned Ground Vehicle Technology III, April 2001, Orlando, FL.
3. H. Komsuoglu, R. Altendorfer, R. Full, U. Saranli, B. Brown, D. McMordie, E. Moore, M. Buehler, and D. Koditschek, "Evidence for Spring Loaded Inverted Pendulum Running in a Hexapod Robot," Int. Symp. Experimental Robotics, Honolulu, HI, Dec 2000.
4. U. Saranli, M. Buehler and D. E. Koditschek, "Design, Modeling and Preliminary Control of a Compliant Hexapod Robot," IEEE Int. Conf. Robotics and Automation, p. 2589-2596, San Francisco, California, April 2000.
5. U. Saranli, M. Buehler, and D. E. Koditschek, "RHex: A Simple and Highly Mobile Hexapod Robot," Int. J. Robotics Research, 20(7):616-631, July 2001.
6. M. Buehler, U. Saranli, D. Papadopoulos and D. E. Koditschek "Dynamic Locomotion with four and six-legged robots," Int. Symp. Adaptive Motion of Animals and Machines, Montreal, Canada, Aug 2000.